IMPEDANCE CONTROL METHOD OF ROBOTIC ARM BASED ON RADIAL BASIS FUNCTION NEURAL NETWORK UNDER THE UNCERTAIN CONDITION OF ENVIRONMENTAL INFORMATION

Xingrui Li*

Abstract

Because of its many benefits, including great production efficiency and high precision machining, mechanical arms are utilised extensively in many different sectors. However, the deployment of compliant control faces obstacles as production activities become more complicated. To address the aforementioned problems, the study first models the pertinent models and the robotic arm's impedance models. It next suggests a radial basis function neural network (RBFNN)-based impedance control technique for the robotic arm to enhance the control's transient performance. Lastly, the challenge of determining reference trajectories under unknown environmental information situations is addressed by an impedance control approach for robotic arms that is based on reference trajectory generation and environment estimating methods. According to the study findings, the contact force effect is reduced to 7.98N under the same conditions when using the RBFNN impedance control approach for robotic arms. The reference trajectory value obtained when the control system is stable is 0.0502 m in the impedance control method of a robotic arm based on reference trajectory generation and environment estimation algorithms; the maximum overshoot of the actual contact force at the end of the robotic arm is 2.1 N. The contact force stays constant after 2.53 s, and the associated error also stabilises at 0. In conclusion, the suggested approach has successfully raised robotic arms' compliance control performance in the face of erratic environmental information.

Key Words

1. Introduction

With the advances in intelligence technology, the industrial scale of the robotic arm has shown explosive growth, and people are more looking forward to the integration of the robotic arm and the environment interaction work scene [1]–[3]. However, in practical applications, if the environment has a large stiffness, even a small positional error will generate a huge contact force, leading to the destruction of the robotic arm and even causing safety accidents [4]. To realise the interaction in the robot arm and the environment, it is necessary to control the position and force of the robot arm at the same time, and this kind of control is the flexible control, which has better application effect under the condition of environmental information determination [5], [6]. However, in general applications, it is difficult to accurately obtain the environmental information of the robotic arm, and at the same time, there are unknown dynamics and information in the dynamics model of the robotic arm, which brings great obstacles to the supple control. Radial basis function neural network (RBFNN) has advantages in approximation ability, learning speed, *etc.*, and can overcome the local minima problem [7]. To address the above problems, the research firstly proposes an impedance control method based on RBFNN robotic arm. Additionally, research is being done to build an impedance control approach for robotic arms based on the environmental estimation algorithm (EEA) (Algorithm Based on Reference Trajectory Generation and Environment Estimation, RTGEE) in order to enhance the control system. The research aims to realise the active and supple control of the robotic arm under the condition of uncertain environmental information, to obtain the

* Department of Mechanical and Electrical Engineering, Hebi Vocational College of Energy and Chemistry, Hebi, Henan 458000, China Corresponding author: Xingrui Li

control function of the CF at the end of the robotic arm, and to improve the competitiveness of the equipment manufacturing and service industries. There are two main innovations in the research, the first one is to propose an adaptive robotic arm impedance control method based on RBFNN to improve the transient performance, and the second one is to design an RTGEE robotic arm control method for determining the reference trajectory. The structure of the study is divided into four main parts, the first part is a review of the relevant research results; the second part is the design of the RBFNN robotic arm impedance control method and the RTGEE robotic arm impedance control method; the third part is the validation of the validity of the proposed method of the study; and the last part is the summary of the study.

2. Related Work

In today's increasingly competitive equipment manufacturing industry and the growing demand of the service industry, robotic arms have received extensive attention from many scholars. Chen *et al.* combined the computer vision system with tracking algorithms to propose a 3D printer-based robotic arm and design mechatronic intelligent vehicle systems. The study assists the robotic arm to detect the color and position of the target through the computer vision system, and the results show that the accuracy gap of target tracking expands from 75.2% to 89.0% [8]. Xu *et al.* constructed an improved artificial potential field method for the traditional artificial potential field for the local minima and other problems, compared with the fast exploratory stochastic tree-based. The algorithm shortens the planning path distance by 13%~41%, and the planning efficiency is significantly improved [9]. Sadiq *et al.* designed a new joint space trajectory tracking controller to solve the influence of unknown dynamic parameters and external interference of the robotic arm, and the robotic arm control can effectively compensate for nonlinear links including friction, friction, *etc.*, in the absence of precise system parameters. The controller is robust to load variations [10]. In order to accurately guide the robotic arm, the path planning has been upgraded to optimise the motion of the robotic arm, and Sharaf *et al.* proposed an improved ant colony optimisation algorithm to obtain the optimal path planning to satisfy the motion objective, and the results of the study confirms the accuracy and efficiency to achieve the optimal paths and trajectories [11].

Nowadays, production activities increasingly require contact between the robotic arm and the environment or the object to be operated, and the size of the CF will determine the quality of the operation and the success of the operation, and it is also the main method to realise the suppleness control, so the impedance control and suppleness control have received widespread attention by the researchers. Rui *et al.* discussed a force-based active suppleness control method for a hydraulic quadrupedal robot, and the joint simulation results show that the robot has a good suppleness, which can realise stable trotting.

The robot has good suppleness and can realise stable trotting [12]. Wang *et al.* found that the concentrated negative sequence current can cause significant torque pulsation in the drive train of a fixed-speed induction generator, which may exceed the stress tolerance of the drive train, so the research proposes a novel hybrid virtual impedance control method, and the theoretical analysis and simulation results validate the operation and performance of this strategy performance [13]. Hanafusa *et al.* aimed to help robots move objects quickly and accurately while maintaining mechanical impedance control. Therefore, a collaborative robot mechanical impedance control method based on recurrent neural network external force estimation is proposed, this method is proved through six degree of freedom experiments [14]. Mokhtari *et al.* [15] to improve the robustness and eliminating jitter, they design a hybrid backpropagation based non-singular fast terminal integral sliding mode control and impedance control scheme, and the simulation results confirm the superiority of this control scheme.

Synthesising the above research results, it can be concluded that the current research focuses on the robotic arm with impedance control under the given conditions, and lacks the relevant research on the robotic arm under the uncertainty of environmental information tuning. To realise the supple control under the condition of uncertain environmental information, the research designed the impedance control method of RBFNN with RTGEE robotic arm.

3. Design of Impedance Control Methods for RBFNN and RTGEE Robotic Arms

For the impedance control problem of robotic arm, the study firstly models the robotic arm related model and impedance model, then designs the RBFNN robotic arm impedance control method, and finally improves the control system and designs the RTGEE robotic arm impedance control method.

3.1 Construction of Robotic Arm Correlation Model and Impedance Model

The robotic arm is a very complex control system whose dynamics is characterised by multiple inputs, multiple outputs, time-varying, strong coupling and nonlinearity, and whose kinematics reveals the interrelationships between the corresponding states of the joints and the end-effector [16], [17]. The kinematics of the robotic arm is modelled as follows: for a robotic arm with m joints, the corresponding joint angle positions are $a \in R^m$ and the end-effector positions are $U \in R^3$ in the Cartesian space. If a is known, the forward kinematics represented by the nonlinear function f can be used to determine U. When performing the modelling, the D–H is usually used to obtain, according to the inverse kinematics can be converted from U to a, and then the derivation can be performed to obtain the velocity mapping relationship between the joint and the Cartesian space, and the
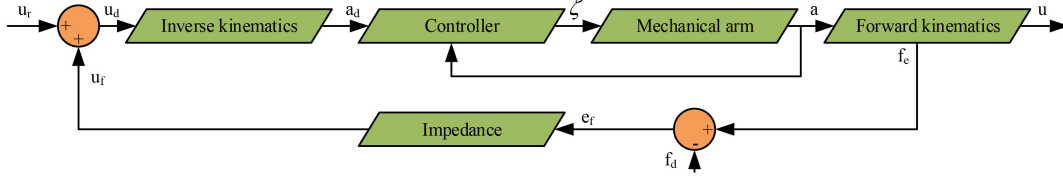
Figure 1. Flowchart of PIC.

calculation is shown in (1).

$$
\begin{cases}
a = f^{-1}(U) \\
\dot{u} = J(a)\dot{a} \\
J(a) = \frac{\partial f(a)}{\partial a}
\end{cases}
\tag{1}
$$

In (1) $J(a) \in R^{3 \times m}$ represents the Jacobi matrix of the robotic arm. The utilitarian model of the robotic arm is then modelled using the Lagrange–Euler equations, and the expression for the robotic arm is (2).

$$
M(a)\ddot{a} + C(a, \dot{a})\dot{a} + G(a) = \zeta
\tag{2}
$$

In (2), $a, \dot{a}, \ddot{a} \in R^m$ is the joint angular position, angular velocity, and angular acceleration, $M(a), C(a, \dot{a}) \in R^{m \times m}$ is the positive definite inertia matrix, centrifugal force term, and Koch's force term, $G(a) \in R^m$ represents the positive definite gravity term, and ζ is the control torque acting on each joint. However, in practical applications, the robotic arm is subject to uncertainties such as external perturbations and inaccurate nominal data, resulting in a less effective control system. Therefore, the study optimises the parameters of the physical characteristics of the robotic arm and is affected by the joint friction $f_n(\dot{a}) \in R^m$ and external perturbation ζ_d during the motion process, which results in the optimised dynamics model as (3).

$$
\begin{cases}
M_0(a)\ddot{a} + C_0(a, \dot{a})\dot{a} + G_0(a) + \zeta_d + f_n(a) + \zeta_\Delta = \zeta \\
\zeta_\Delta = \Delta M(a)\ddot{a} + \Delta C(a, \dot{a})\dot{a} + \Delta G(a)
\end{cases}
\tag{3}
$$

In (3), M_0, C_0 and G_0 stand for the nominal parameters. ΔM, ΔC and ΔG stand for the positional deviations of the nominal values from the real values. Let the states of the robotic arm be $u_1 = a$ and $u_2 = \dot{a}$, then substitute u_1 and u_2 into (3), and simplify and transfer formulas (1) and (2) simultaneously. Finally, the obtained $\dot{u}_1$ and $\dot{u}_2$ are placed on the left side of the equation to obtain the state space equation. The calculation is shown in (4).

$$
\begin{cases}
\dot{u}_1 = u_2 \\
\dot{u}_2 = M_0^{-1}(\zeta - \zeta_\Delta - \zeta_d - C_0 u_2 - G_0 - f_n)
\end{cases}
\tag{4}
$$

After the robot arm related model is completed, the modelling of the impedance control model is divided into position-based impedance control (PIC) and force-based impedance control (FIC) [21], [22]. Among them, PIC

converts the contact force error into a correction for the reference trajectory based on the given impedance relationship, then controls the robotic arm to move along the corrected path, and finally achieves control of the docking contact force. Figure 1 displays the flowchart of PIC.

Based on the above principle, the transfer function expression for the impedance part is (5).

$$
u_f(g) = \frac{1}{kg^2 + bg + h} e_f(g)
\tag{5}
$$

In (5), k, b, and h correspond to the inertia coefficients, damping coefficients, and stiffness coefficients of the impedance relationship. e_f stands for the contact force error in the corresponding direction. The CF between the end of the robotic arm and the environment is generated by the deformation of the environment, and usually the spring model is chosen for modelling the contact force, and the calculation is shown in (6).

$$
f_e =
\begin{cases}
h_e(u_e - u), & u < u_e \\
0, & u \geq u_e
\end{cases}
\tag{6}
$$

In (6), h_e and u_e are the ambient stiffness and ambient position, respectively. Neglecting the error of the robotic arm position control, we can get e_f in the specified direction, see (7).

$$
e_f = \frac{(kg^2 + bg + h)[h_e(u_e - u_r) - f_d]}{kg^2 + bg + h + h_e}
\tag{7}
$$

In (7), u_r represents the actual position of the robot arm in the specified direction, and f_d represents the given desired contact force in the specified direction. The steady state error can be calculated by classical control theory, see (8).

$$
e_{f_n} = \frac{h[h_e(u_e - u_r) - f_d]}{h + h_e}
\tag{8}
$$

In practice, it is very difficult to obtain the environmental parameters accurately, so other methods are used to generate the reference trajectory or the output of the compensated impedance. The FIC works as shown in Fig. 2.

In Fig. 2, the error between the end position and the reference trajectory e_u is firstly detected, and secondly converted into a correction of the desired force by impedance Δf, and at the same time superimposed with the reference contact force f_r to obtain f_d, and finally, the difference between f_d and the actual CF is used as an input
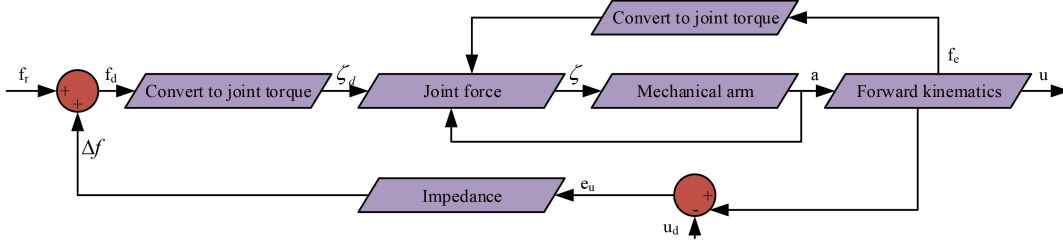
3

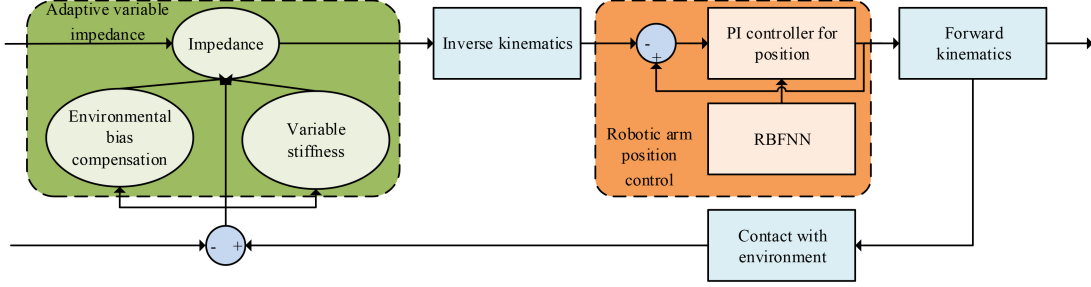Figure 2. Schematic diagram of the working principle of FIC.

Figure 3. Flowchart of adaptive robotic arm impedance control method based on RBFNN.

to the moment controller of the robotic arm, which enables the trajectory error to be converted into an adjustment of the force.

3.2 RBFNN-based Impedance Control Method for Robotic Arm

To realise the end CF control of the robotic arm under the condition of uncertain environmental information, the variable impedance method is the mainstream method at present, but its transient performance cannot be guaranteed due to the parameter change, which makes the robotic arm and the environment contact with a large contact force impact [23]. To address the above problems, the study proposes an adaptive robotic arm impedance control method based on RBFNN, and the specific flow is shown in Fig. 3.

In Fig. 3, firstly, the PD iterative method is used to compensate for the estimation error of the environment, in order to provide high impedance control for robustness in uncertain environments; Secondly, the variable stiffness impedance method is used to reduce excessive contact force impact during contact, and the gradient descent method is used to solve the impedance change. Then, to address the errors caused by parameter disturbances, external disturbances, and other factors, a position based PI controller was designed. Finally, RBFNN was used to approximate the uncertain part of environmental information in the dynamics of the robotic arm. In this case, the variable stiffness impedance algorithm is operated as follows, according to the impedance relationship in the specified direction in Cartesian space, the expression can be obtained as (9).

$$k\left(\ddot{u} - \ddot{u}_r\right) + b\left(\dot{u} - \dot{u}_r\right) + h\left(u - u_r\right) = f_e - f_d = e_f \quad (9)$$

In (9), u, $\dot{u}$, and $\ddot{u}$ stand for the actual position, velocity, and acceleration of the end of the robot arm, while u_r, $\dot{u}_r$, and $\ddot{u}_r$ are the reference trajectory, velocity, and acceleration. To minimise the influence of the positional error of the robot arm on the contact force control, it is assumed that the end of the robot arm can accurately track the desired position. The environmental position $\widehat{u}_e$ is obtained through the sensor measurement, which corresponds to the given reference trajectory as follows, $u_r = \widehat{u}_e$. The error in the measured value and the real value is expressed as ψu_e, which leads to the impedance model; then define $\psi\left(t\right) = k\psi\ddot{u}_e + b\psi\dot{u}_e + h\psi u_e$, which leads to (10).

$$k\ddot{\widehat{e}} + b\dot{\widehat{e}} + he + \psi\left(t\right) = f_e - f_d = e_f \quad (10)$$

To compensate the effect of environmental errors on the control system, the study introduces the PD iterative method and designs the compensation amount as (11).

$$\psi\left(t\right) = \psi\left(t - \tau\right) + \sigma\left[f_d\left(t\right) - f_e\left(t\right)\right]$$
$$+ \frac{\vartheta}{\psi}\left\{\begin{array}{c}\left[f_d\left(t\right) - f_e\left(t\right)\right] \\ -\left[f_d\left(t - \tau\right) - f_e\left(t - \tau\right)\right]\end{array}\right\} \quad (11)$$

In (11), τ represents the sampling period. σ and ϑ represent the positive definite learning rate. To improve the adaptability of the control system to the changing environment, the study adds the variable impedance mechanism, defines the stiffness variation as h_v, and defines $h_v\widehat{e} = f_0$, which leads to (12).

$$\begin{cases}\dot{\widehat{e}} = \frac{\left[e_f - k\ddot{\widehat{e}} - h\widehat{e} - \psi(t) - f_0\right]}{b} \\ \ddot{u}_d = \ddot{\widehat{u}} + \frac{\left[e_f - b\dot{\widehat{e}} - h\widehat{e} - \psi(t) - f_0\right]}{k}\end{cases} \quad (12)$$
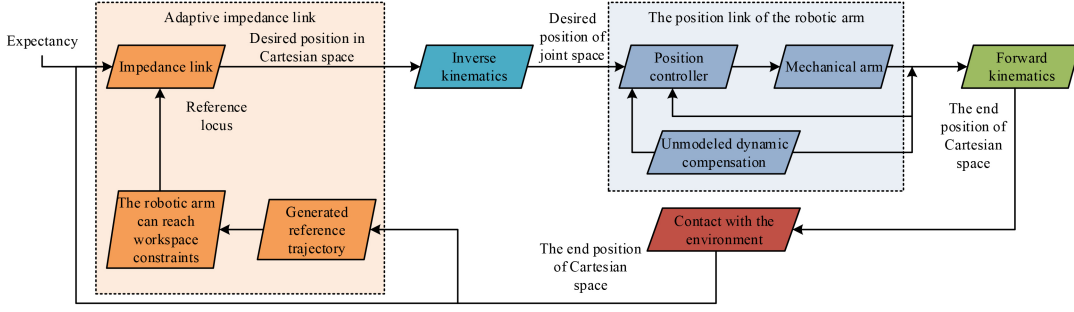
4

Figure 4. Schematic diagram of impedance control method flow for RTGEE robotic arm.

To achieve the control objective of minimising the position error and contact force error, the study introduces an optimisation method, and the objective equation of the optimisation is selected as (13).

$$Q(t) = \frac{1}{2}\left(\lambda \dot{\hat{e}}^2 + \eta e_f^2\right) = \frac{1}{2}(f_1 + f_2) \quad (13)$$

To minimise the value of (13), it is necessary to make f_0 follow the gradient in the opposite direction, see (14).

$$f_0(t) = f_0(t - \tau) - \beta \nabla Q \quad (14)$$

In (14) β represents the step size of the change. In the PI controller part of the control method, the joint angle position error is derived in time and the generalised tracking error is defined according to the dynamics model of the robotic arm with the state space equations, see (15).

$$\begin{cases} \dot{e} = \dot{a}_d - u_2 \\ r = \dot{e} + e \end{cases} \quad (15)$$

In (15) denotes the positive definite diagonal matrix. Deriving (15) with respect to time and multiplying it with M_0 at the same time leads to (16).

$$\begin{aligned} M_0 \dot{r} =\ & M_0(\ddot{a}_d + \dot{e}) + C_0 r + C_0(\dot{a}_d + e) \\ & + G_0 + \zeta_\Delta - \zeta + f_n + \zeta_d \end{aligned} \quad (16)$$

The control law is designed as (17).

$$\begin{aligned} \zeta =\ & M_0(\ddot{a}_d + \dot{e}) + C_0(\dot{a}_d + e) + G_0 + \zeta_\Delta + f_n(\dot{a}) \\ & + \zeta_d + M_P r + M_i \int r \mathrm{d}t \end{aligned} \quad (17)$$

In (17) $M_P, M_i \in R^{m \times m}$ all denote positive definite diagonal matrices. Estimating the positional part of (17) using the universal approximation property of the RBFNN leads to (18).

$$\begin{aligned} \zeta =\ & M_0(\ddot{a}_d + \dot{e}) + C_0(\dot{a}_d + e) + G_0 + M_P r \\ & + M_i \int r \mathrm{d}t + \widehat{W}^T l(\theta) + M_r \mathrm{sgn}(r) \end{aligned} \quad (18)$$

In (18), denotes the weights of the RBFNN, $\theta = (e, \dot{e}, a_d, \dot{a}_d, \ddot{a}_d)^T$ and $l(\cdot)$ represent the inputs and outputs of the RBFNN, and M_r is a positive definite diagonal

matrix. The adaptive law of the RBFNN is designed as (19).

$$\dot{\hat{w}} = \Gamma^{-1} l r^T \quad (19)$$

In (19) Γ represents the positive definite diagonal matrix.

3.3 Design of Impedance Control Method for Robotic Arm Based on Reference Trajectory Generation and Environment Estimation Algorithm

The impedance control of the robotic arm needs to take the contact force error and the reference trajectory as inputs, but it is difficult to generate the reference trajectory under the condition of uncertain environmental information [24]–[26]. Aiming at the problems of impedance control of the control system, research and design an RTGEE robotic arm impedance control method, the specific flow is shown in Fig. 4.

In Fig. 4, the EEA algorithm is first used to estimate environmental information and calculate the reference trajectory using the obtained information. If the generated reference trajectory is outside the range of the workspace that the robotic arm can reach, it can be constrained to the farthest distance that can be reached. The constrained reference trajectory can be corrected through the impedance link to obtain the desired position, solving the problem of the control system being unable to accurately adjust the end position. Secondly, the desired position is obtained by reversing the desired angular position in the joint space with inverse motion, and at the same time constructing a fixed-time and stable position controller to track the desired angular position. Finally, the algorithm for compensating unmodelled dynamics of robotic arms (CUDRA) is designed to reduce the effect of unknown conditions of the robotic arm model on the unknown control. According to the EEA algorithm proposed in the study, by defining the end contact force, environmental parameters can be estimated, and the derivation can be obtained as (20).

$$\widehat{f}_e = \widehat{h}_e(\widehat{u}_e - u_d) \quad (20)$$

In (20), $\widehat{f}_e$ is the estimated value of CF, and $\widehat{h}_e$ and $\widehat{u}_e$ are the estimated environmental stiffness and environmental position. $\widehat{f}_e$ The difference in this value and
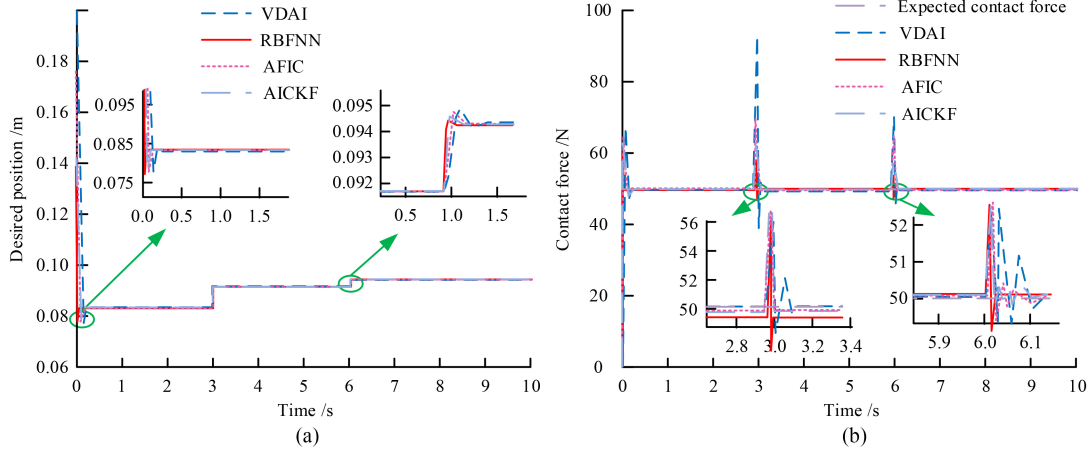
Figure 5. Expected position and contact force generated by different methods for contact force control on a variable stiffness plane: (a) Desired location and (b) Contact force.

the measured value f_e is shown in (21).

$$\widehat{f}_e - f_e = \left(\widehat{h}_e \widehat{u}_e - h_e u_e\right) - \left(\widehat{h}_e - h_e\right) u_d \qquad (21)$$

According to the theory of Lyapunov stability in order to determine the estimation of environmental parameters, the Lyapunov function is shown in (22).

$$L = \frac{1}{2\gamma_1}\left(\widehat{h}_e - h_e\right)^2 + \frac{1}{2\gamma_2}\left(\widehat{h}_e \widehat{u}_e - h_e u_e\right)^2 \qquad (22)$$

In (22), $\gamma_1, \gamma_2 \in R$ is a normal number. Normally, $\widehat{f}_e$ and f_e will have some error, so the reference trajectory is designed as (23).

$$u_r = \widehat{u}_e - \frac{f_d}{\widehat{h}_e} \qquad (23)$$

The specific operation process of the CUDRA algorithm is as follows. Firstly, a compensation term q is designed to compensate for the unmodelled dynamics in the dynamic model of the robotic arm. When the control input simultaneously acts on the real and compensated robotic arm models, it can generate two operating speeds: reference and real. If the effect of compensating for unmodelled dynamics is not complete, there will be significant errors in the two sets of outputs. Therefore, the feedback control concept is introduced to use the generated errors as feedback and compensate in the control law to reduce the adverse effects caused by unmodelled dynamics. Secondly, in the position controller of the robotic arm control system, the desired position obtained is taken as input, and then using (4), the parameter perturbation part, external disturbance part, and joint friction are all treated as unmodelled parts. Finally, to improve the convergence speed of the controller and enable the robotic arm to better meet the requirements of contact force control, the idea of backstepping is introduced, and an adaptive position control algorithm that can converge in a fixed time is used.

4. Analysis of Results of Impedance Control Methods for RBFNN and RTGEE Robotic Arms

To verify the effectiveness of the proposed method for robotic arms and the RTGEE robotic arm impedance control method, simulation verification was conducted through plane, oscillation surface, and environmental information uncertainty conditions.

4.1 Result Analysis of RBFNN-based Impedance Control Method for Robotic Arm

To verify the effectiveness of the impedance control method of the RBFNN robotic arm, the study firstly verifies the CF control on the plane. The desired force is 50 N, the environment position is 0.1 m, the initial position is 0.2 m, the reference trajectory is 0.05 m, $k = 1$, $b = 120$, $h(0) = 100$, $\sigma = 0.5$ and $\vartheta = 0.4$. In addition, to scientifically validate the effectiveness of the proposed method, the study selected variable damping adaptive impedance (VDAI), adaptive fuzzy impedance control (AFIC), and adaptive impedance control based on Kalman filter (AICKF) for comparative experiments.

The results of the desired position and CF produced by the different methods for contact force control in the variable stiffness plane are displayed in Fig. 5. As shown in Fig. 5, if the reference trajectory is only the estimated environmental position, all four control methods can respond quickly and obtain the most suitable expected position. But a sudden change in environmental stiffness was set in the 3rd and 6th seconds, resulting in significant jumps at these two moments. When the robotic arm using VDAI algorithm comes into contact with the environment or experiences sudden changes in the environment, it will generate the maximum contact force impact, which is 52.03 N; the maximum contact impact forces generated by AFIC algorithm and AICKF algorithm are 51.83 N and 50.16 N, respectively. The impedance control method of RBFNN robotic arm can reduce the contact force impact to 7.98 N under the same conditions. The above results indicate that
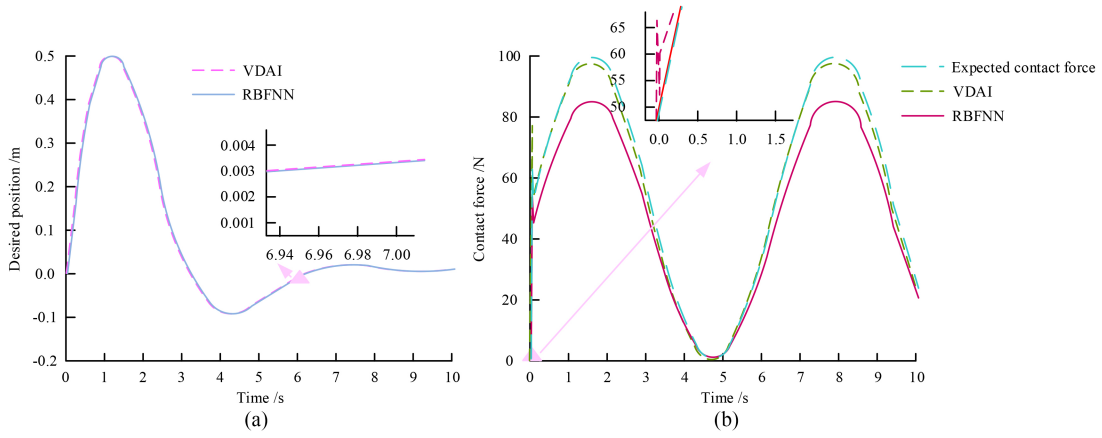
Figure 6. The expected position, actual CF, and contact force error results of the expected force generated by tracking changes using different methods on the attenuated oscillation surface: (a) Desired location and (b) Contact force.
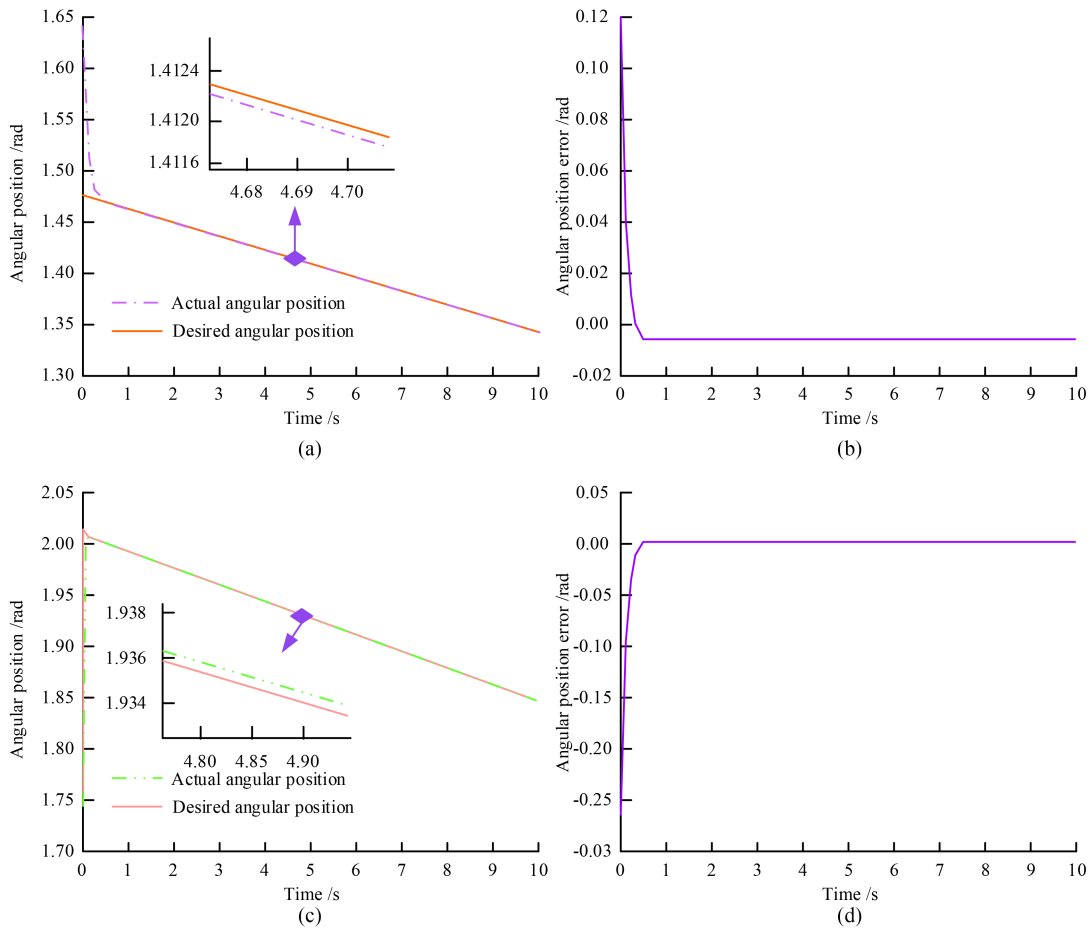

Figure 7. Angular position and position error results of robotic arm joints 1 and 2: (a) angular position of joint 1; (b) angular position error of joint 1; (c) angular position of joint 2; and (d) angular position error of joint 2.

the proposed RBFNN control method can quickly change the impedance relationship when the environment changes, control the contact force impact within a small range, avoid damage to objects, and ensure the stability of the robotic arm operation. The second study verifies the effectiveness of the different methods in controlling the varying desired contact force on an oscillating surface, with the following parameter settings and the environment true position is

$e^{-\frac{t}{2}} \sin(t)$, desired force is $50 + 50 sin(t)$, ambient stiffness is 5000 N/m, the initial position is 0, $k = 1$, $b = 90$, $h(0) = 50$, $\sigma = 0.6$ & $\vartheta = 0.4$.

The results of tracking the desired position, actual contact force and contact force error generated by different methods of tracking the changing desired force on the decaying oscillating surface are displayed in Fig. 6. Figure 6 displays that, although the VDAI method can
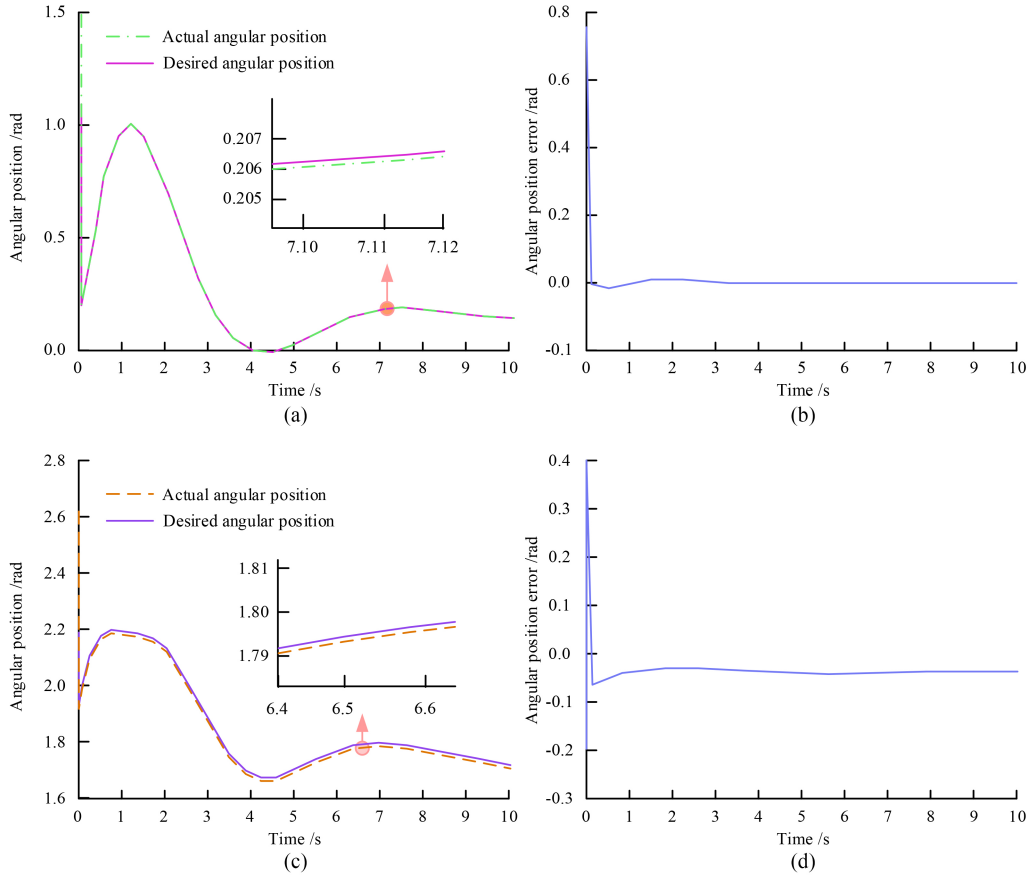
Figure 8. Angular positions and error results of two joints under the oscillating surface: (a) angular position of joint 1; (b) angular position error of joint 1; (c) angular position of joint 2; and (d) angular position error of joint 2.
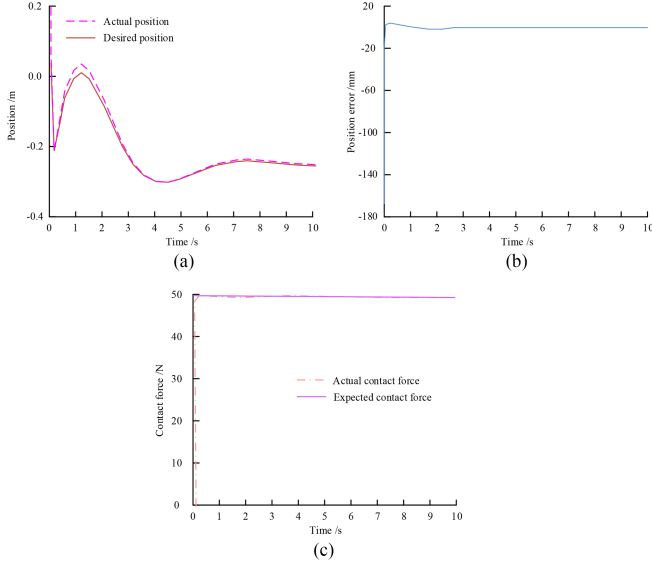

Figure 9. Control effect of the robotic arm on the Y-axis direction under the oscillating surface.

control the steady state error of the CF within a certain range, it still causes a large force shock and has a large fluctuation of change in 4 s. The AFIC method and AICKF method can control the steady-state error of contact force within a small range, but there is still a certain degree

of fluctuation. The impedance control method of RBFNN robotic arm reduces the impact of contact force by 17 N through automatic adjustment of impedance relationship and constraint of contact force error. The above results indicate that the proposed method can effectively avoid significant contact force fluctuations and has good control effects. To further verify the overall contact force control effect of the robotic arm control system, a planar two-link robotic arm is used for simulation. The simulation scenario is a uniform motion in the plane X-axis direction according to the speed of 0.0055 m/s, and the CF is controlled in the Y-axis. The simulation parameters are set as follows, the real position of the environment is 0.2 m, the reference trajectory is set to 0.016 m, the environment stiffness is 5000 N/m, and the desired CF is 50 N The initial position of the end of the robot arm is (0.3 m, 0.3 m). The parameters in the controller are as follows, the implicit layer and the output node of the RBFNN are set to 7 and 2, respectively, $k = 1$, $b = 120$, $h(0) = 100$, $\sigma = 0.1$, $\vartheta = 0.4$, $= \text{diag}(10, 50)$, $M_p = \text{diag}(200, 200)$, $M_i = \text{diag}(100, 100)$, $M_r = \text{diag}(3, 3)$ and $\Gamma = \text{diag}(0.2, 0.2)$.

The results of the angular position and position error of joints 1 and 2 are shown in Fig. 7. Figure 7 displays the error between the two joints of the robotic arm and the actual position is small, and the angular error of the two joints is stabilised at 0 rad within 0.5 s. The control system is still able to respond quickly although the robotic arm inevitably generates errors.
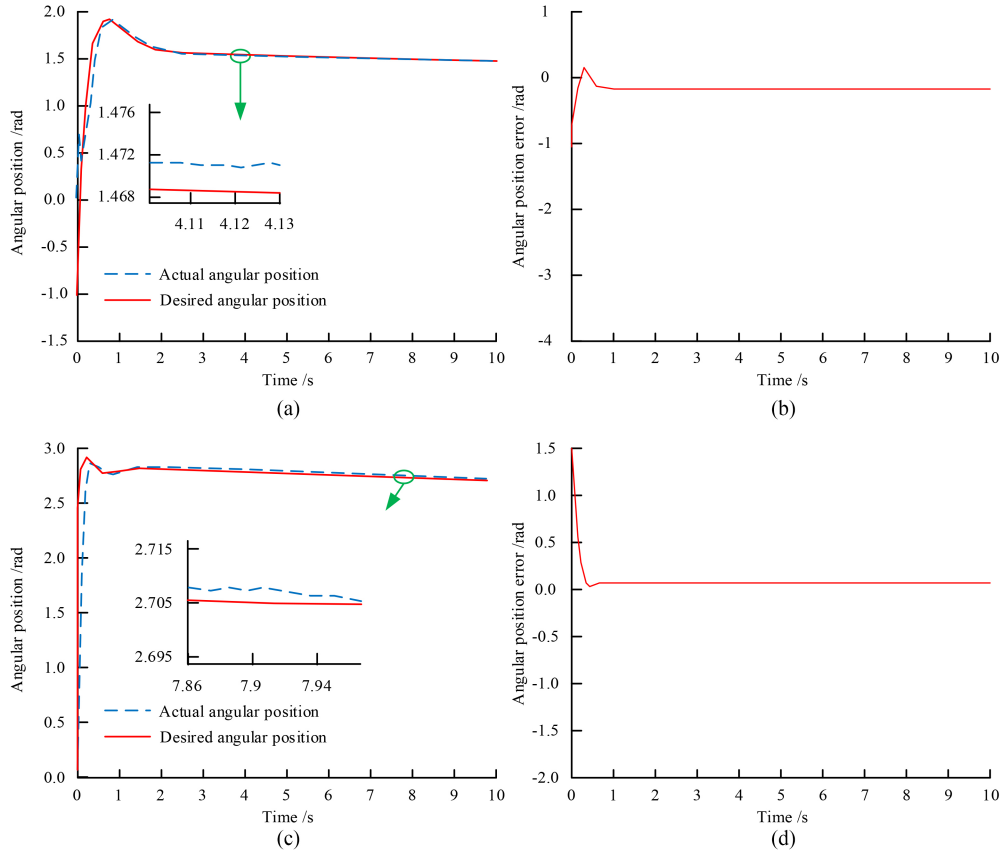
Figure 10. Expected angle position and tracking error results of two joints based on RTGEE robotic arm impedance control method; (a) angular position of joint 1; (b) angular position error of joint 1; (c) angular position of joint 2; and (d) angular position error of joint 2.

Table 1
Control Effect of the Robotic Arm in the Y-axis Direction

Attribute	Project	Time/s										
		0	1	2	3	4	5	6	7	8	9	10
Position	Desired position/m	0.19	0.19	0.19	0.19	0.19	0.19	0.19	0.19	0.19	0.19	0.19
	Actual position/m	0.30	0.19	0.19	0.19	0.19	0.19	0.19	0.19	0.19	0.19	0.19
Y-axis position error	Position Error/mm	110	0	0	0	0	0	0	0	0	0	0
Contact force	Expected contact force/N	50	50	50	50	50	50	50	50	50	50	50
	Actual contact force/N	0	50	50.5	50.5	50.5	50.5	50.5	50.5	50.5	50.5	50.5
Contact force error in Y-axis direction	Contact force error/N	50	0	−0.5	−0.5	−0.5	−0.5	−0.5	−0.5	−0.5	−0.5	−0.5

Table 1 displays the control effect of the robotic arm in the Y-axis direction. It displays that the position control of the robotic arm can be stabilised within 1 s, and the steady state error in Cartesian space is within 0.15 mm; and the steady state error of the CF is within 0.5 N. To validate the robustness in the dynamic environment, the study sets the simulation environment as an oscillating surface, and the robotic arm is moving at a speed of 0.005 m/s. The simulation parameters are as follows: The environment stiffness is 200 N/m, the reference trajectory is $0.7 \times \exp\left(-\frac{t}{2}\right) \times \sin(t)$, the initial position is (0.3 m,

0.2 m), and the desired CF is 50 N, $b = 90$, $h(0) = 50$, $\sigma = 0.6$, $\vartheta = 0.4$. The position controller parameters are $= \operatorname{diag}(80, 80)$, $M_p = \operatorname{diag}(60, 60)$, $M_i = \operatorname{diag}(30, 30)$, $M_r = \operatorname{diag}(3, 3)$ and $\Gamma = \operatorname{diag}(3, 3)$. The results of the angular position and error of the two joints under the oscillating surface are displayed in Fig. 8. From Fig. 8, the angular position error of joint 1 is very small, fluctuating in the range of 0.02 rad and stabilising to 0 after 2.5 s. The angular position error of joint 2 has a larger band, fluctuating around 0.03 rad and stabilising to 0 after 4 s. The angular position error of joint 2 is also larger,
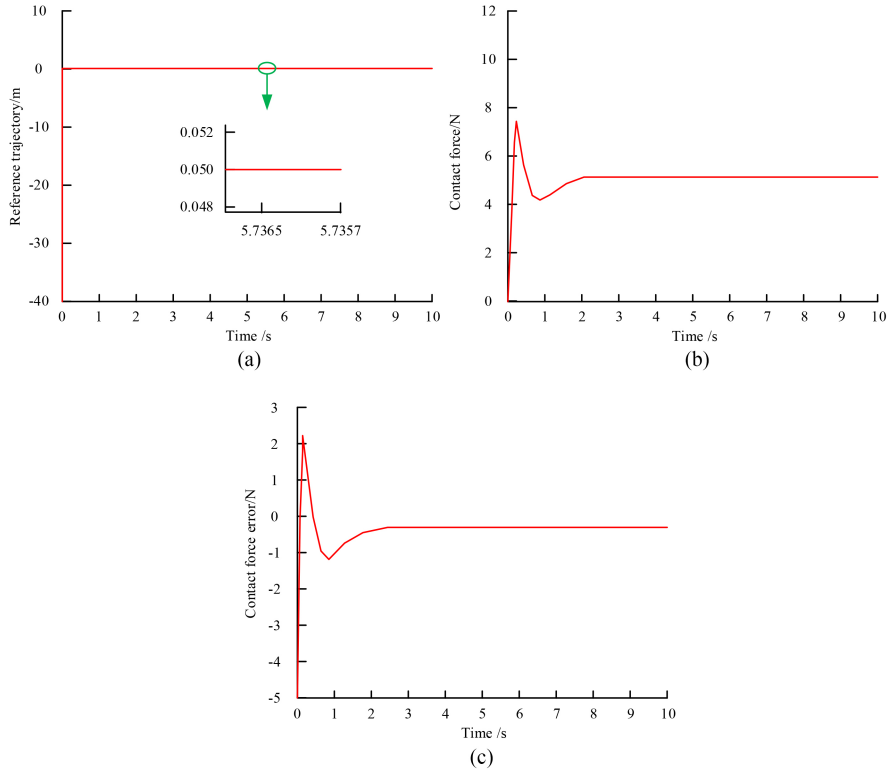
Figure 11. The reference trajectory obtained through estimated environmental information calculation and the actual CF and contact force error curve at the end of the robotic arm: (a) Reference trajectory obtained by calculating estimated environmental information; (b) actual contact force at the end of the robotic arm; (c) Contact force error at the end of the robotic arm.

fluctuating near 0.03 rad and stabilising to 0 after 4 s. The angular position of joint 2 is also larger than that of joint 2.

The control effect of the robotic arm in the Y-axis under the oscillating surface is shown in Fig. 9. Figure 9 shows that the contact between the robotic arm and the environment can be generated within 0.2 s, and at the same time, the generated desired position can be tracked quickly. The whole control system can reach a smooth state within 3 s, and only generates oscillation and overshoot in the range of 3 mm, and the position error and contact force error are 0.18 mm and 0.25 N, respectively, after reaching a stable state. The above results validate the effectiveness of the proposed algorithm. Under uncertain conditions, the algorithm can effectively reduce the force impact when the robotic arm contacts the environment, improve the transient performance of impedance control, and ensure the performance and stability of robotic arm operation.

4.2 Analysis of Results of RTGEE Robotic Arm Impedance Control Methods

To verify the performance of the RTGEE robotic arm impedance control method, the study is simulated using a planar two-link robotic arm, and the simulation environment is consistent with the above. The unknown external perturbation is $0.1\sin(t)$, the true environmental position is 0.3 m, the desired force is 5 N, the environmental stiffness is 20 N/m, and the initial position in Cartesian

space is (0.3 m, 0.3 m). $k = 1$, $b = 10$, $h(0) = 1$, and the initial values of the environmental stiffness and position are 0.1 m.

The results of the desired angular position and tracking error of the two joints against the desired angle based on the RTGEE robotic arm impedance control method are displayed in Fig. 10. From Fig. 10, in the primary stage of applying the control action, there is a small amplitude of oscillation and overshooting at the two joints, and the position error of the two joints stabilises at 0 rad after adjustment.

The reference trajectory obtained by calculating the estimated environmental information and the actual contact force at the end of the robotic arm are displayed in Fig. 11. From Fig. 11, at the beginning of the simulation, the reference trajectory obtained is larger because the initial values of the environmental stiffness and the environmental position are smaller, but the contact force obtained by measurement can be adjusted quickly to the estimated value by the EEA algorithm. When it is stabilised, the value of the obtained reference trajectory is 0.0502 m. At the initial stage, the actual contact force is 0, and then it produces slight oscillations and overshooting with the maximum overshooting amount of 2.1 N. The contact force is in a smooth state after 2.53 s, and the corresponding error is stabilised at the 0 value. The above results demonstrate the effectiveness and stability of the proposed RTGEE impedance control method for robotic arms, which can effectively solve the problems of

contact force control and reference trajectory formulation of robotic arms under uncertain environmental information conditions.

5. Conclusion

With the increasing automation of robotic arms, they are widely used in various fields due to their advantages such as high productivity and the ability to operate in harsh environments. However, in practical applications, the difficulty of obtaining accurate environmental information hinders the flexible control of robotic arms. To address the above problems, the study first models the robotic arm related model and impedance model, then proposes a robotic arm impedance control method based on RBFNN, and finally designs an RTGEE robotic arm impedance control method. In the contact force comparison of different methods, the VDAI algorithm produces the largest contact force impact of 52.03 N. The impedance control method of the robotic arm based on RBFNN reduces the contact force impact to 7.98 N. In the attenuated oscillating surface, the two joints of the robotic arm have a small error from the actual position, and the angular error of the two joints stabilises at 0 rad within 0.5 s. The whole control system under the oscillating surface has the following advantages: In the oscillation surface, the whole control system can reach a smooth state within 3 s, and only produces 3 mm range of oscillation and overshooting, and after reaching the stable state, the position error and contact force error are 0.18 mm and 0.25 N, respectively. In the RTGEE robotic arm impedance control method, when the control system is stabilised, the reference trajectory value obtained is 0.0502 m, and the actual CF is 2.1 mm, the maximum overshooting amount is 2.1 mm. The maximum overshoot is 2.1 N, and the contact force is in a smooth state after 2.53 s, and the corresponding error is stabilised at 0 value. In summary, the proposed method has good performance and can effectively improve the adverse effects on the flexible control of the robotic arm under the condition of uncertain environmental information. However, there are still shortcomings in the study, and the method proposed in the study is only tested in the simulation environment, and an experimental platform can be constructed to verify its effectiveness in practical applications in further studies in the future.

References

[1] Y. Fang, B. Luo, T. Zhao, D. He, B. Jiang, and Q. Liu, ST-SIGMA: Spatio-temporal semantics and interaction graph aggregation for multi-agent perception and trajectory forecasting, *CAAI Transactions on Intelligence Technology, 7*(4), 2022, 744–757.

[2] J. Zan, Research on robot path perception and optimization technology based on whale optimization algorithm, *Journal of Computational and Cognitive Engineering, 1*(4), 2022, 201–208.

[3] P. Dey and D.K. Jana, Evaluation of the convincing ability through presentation skills of pre-service management wizards using AI via T2 linguistic fuzzy logic, *Journal of Computational and Cognitive Engineering, 2*(2), 2022, 133–142.

[4] D.H.T. Nguyen, R.H. Utama, K.C. Tjandra, P. Suwannakot, E.Y. Du, M. Kavallaris, R.D. Tilley, and J.J. Gooding, Tuning the mechanical properties of multiarm RAFT-based block copolyelectrolyte hydrogels, *Biomacromolecules, 24*(1), 2023, 57–68.

[5] M.R. Sarifin, M. Nor, S. Ali, N. Ameera, and I.S. Hamzah, Categories for non-compliance of movement control order in malaysia: A review through online news report, *Psychology (Savannah, Ga.), 57*(8), 2020, 263–290.

[6] C.M. Murea and D. Tiba, Topological optimization and minimal compliance in linear elasticity, *Evolution Equations and Control Theory, 9*(4), 2020, 1115–1131.

[7] Z. Chen, Research on internet security situation awareness prediction technology based on improved RBF neural network algorithm, *Journal of Computational and Cognitive Engineering, 1*(3), 2022, 103–108.

[8] I.Z. Chen and J.T. Chang, Applying a 6-axis mechanical arm combine with computer vision to the research of object recognition in plane inspection, *Journal of Artificial Intelligence and Capsule Networks, 2*(2), 2020, 77–99.

[9] T. Xu, H. Zhou, S. Tan, Z. Li, X. Ju, and Y. Peng, Mechanical arm obstacle avoidance path planning based on improved artificial potential field method, *Industrial Robot, 49*(2), 2022, 271–279.

[10] A.T. Sadiq, F.A. Raheem, and N.A.F. Abbas, Ant colony algorithm improvement for robot arm path planning optimization based on D* strategy, *International Journal of Mechanical & Mechatronics Engineering, 21*(1), 2021, 96–111.

[11] H.K. Sharaf, M.R. Ishak, S.M. Sapuan, N. Yidris, and A. Fattahi, Experimental and numerical investigation of the mechanical behavior of full-scale wooden cross arm in the transmission towers in terms of load-deflection test, *Journal of Materials Research and Technology, 9*(4), 2020, 7937–7946.

[12] Z. Rui, Y. Qingjun, C. Chen, C. Jiang, C. Li, and Y. Wang, Force-based active compliance control of hydraulic quadruped robot, International *Journal of Fluid Power, 22*(2), 2021, 147–172.

[13] T. Wang, H. Nian, and Z. Zhu, Hybrid virtual impedance-based control strategy for dfig in hybrid wind farm to disperse negative sequence current during network unbalance, *IET Renewable Power Generation, 14*(12), 2020, 2268–2277.

[14] M. Hanafusa and J. Ishikawa, Mechanical impedance control of cooperative robot during object manipulation based on external force estimation using recurrent neural network, *Unmanned Systems, 8*(3), 2020, 239–251.

[15] M. Mokhtari, M. Taghizadeh, and P.G. Ghanbari, Fault tolerant control based on backstepping nonsingular terminal integral sliding mode and impedance control for a lower limb exoskeleton. *Proceedings of the Institution of Mechanical Engineers, Part C: Journal of Mechanical Engineering Science, 236*(6), 2022, 2698–2713.

[16] J. Chen, Q. Chen, and H. Yang, Additive manufacturing of a continuum topology-optimized palletizing manipulator arm, *Mechanical Sciences, 12*(1), 2021, 289–304.

[17] H. Yang, S. Wu, and G. Huang, Fuzzy neural network control for mechanical arm based on adaptive friction compensation, *Journal of Vibroengineering, 22*(5), 2020, 1099–1112.

[18] A. Kumar and R. Sharma, Linguistic Lyapunov reinforcement learning control for robotic manipulators, *Neurocomputing, 272*, 2017, 84–95.

[19] A. Kumar and R. Sharma, Fuzzy Lyapunov reinforcement learning for non linear systems, *ISA Transactions, 67*, 2017, 151–159.

[20] A. Kumar and R. Sharma, Neural/fuzzy self learning Lyapunov control for non linear systems, *International Journal of Information Technology, 14*, 2022, 229–242

[21] Z. Lu, P. Huang, and Z. Liu, High-gain nonlinear observer-based impedance control for deformable object cooperative teleoperation with nonlinear contact model, *International Journal of Robust and Nonlinear Control, 30*(4), 2020, 1329–1350.

[22] J. Dong, and J. Xu, Physical human-robot interaction force control method based on adaptive variable impedance, *Journal of the Franklin Institute, 357*(12), 2020, 7864–7878.

[23] X. Zhang, T. Sun, and D. Deng, Neural approximation-based adaptive variable impedance control of robots, *Transactions of the Institute of Measurement and Control, 42*(13), 2020, 2589–2598.

[24] A. Kumar, Reinforcement learning: Application and advances towards stable control strategies, *Mechatronic Systems and Control*, *51*(1), 2023, 53–57.

[25] A.K. Yadav, V. Kumar, A.S. Pandey, S.M. Tripathi, and A. Kumar, Wind farm integrated fuzzy logic-based facts controlled power system stability analysis, *Mechatronic Systems and Control*, *51*(4), 2023, 172–181.

[26] A. Kumar, R. Sharma, and P. Vershey, Lyapunov fuzzy Markov game controller for two link robotic manipulator, *Journal of Intelligent & Fuzzy Systems, 34*(3), 2018, 1479–1490.

Biographies

Xingrui Li received the B.S. and M.S. degrees from the School of Mechanical Engineering, Henan Polytechnic University in 2007 and 2018, respectively. Since 2007, he has been teaching with Hebi Vocational College of Energy and Chemistry, as an Associate Professor. His current research fields include mechanical design and intelligent manufacturing.